Eur J Nucl Med Mol Imaging (2013) 40:1047–1056
DOI 10.1007/s00259-013-2383-1

ORIGINAL ARTICLE

Investigation of ^{90}Y-avidin for prostate cancer brachytherapy: a dosimetric model for a phase I–II clinical study

Francesca Botta · Marta Cremonesi · Mahila E. Ferrari · Ernesto Amato · Francesco Guerriero · Andrea Vavassori · Anna Sarnelli · Stefano Severi · Guido Pedroli · Giovanni Paganelli

Received: 11 October 2012 / Accepted: 26 February 2013 / Published online: 3 May 2013

Abstract
Purpose A novel method for prostate irradiation is investigated. Similarly to ^{125}I or ^{103}Pd seed brachytherapy, ^{90}Y-avidin could be injected via the perineum under ultrasound image guidance. This study inspects the theoretical feasibility with a dosimetric model based on Monte Carlo simulation.
Methods A geometrical model of the prostate, urethra and rectum was designed. The linear-quadratic model was applied to convert ^{125}I absorbed dose prescription/constraints into ^{90}Y dose through biological effective dose (BED) calculation. The optimal ^{90}Y-avidin injection strategy for the present model was obtained. Dose distribution was calculated by Monte Carlo simulation (PENELOPE,GEANT4). Dose volume histograms (DVH) for the prostate, urethra and rectum were compared to typical DVHs of ^{125}I seed brachytherapy, used routinely in our institute.
Results With ^{90}Y-avidin, at least 95 % of the prostate must receive more than 70 Gy. The absorbed dose to 10 % of the urethra ($D_{10\%\_urethra}$) and the maximum absorbed dose to the rectum (D_{max_rectum}) must be lower than 122 Gy. For the present model, the optimum strategy consists in multiple injections of ^{90}Y-avidin 50 μl drops, for a total volume of 3.1 ml. The minimum activity to deliver the prescribed absorbed dose is 0.7 GBq, which also fully respects urethral and rectal constraints. The resulting dose map has a maximum in the central region with a sharp decrease towards the urethra and the prostate edge. Notably, $D_{10\%\_urethra}$ is 95 Gy and D_{max_rectum} is below 2 Gy. Prostate absorbed dose is higher with ^{90}Y-avidin than ^{125}I seeds, although the total volume receiving the prescribed absorbed dose is 1–2 % lower. Urethral DVH strictly depends on the ^{90}Y distribution, to be optimized according to prostate shape; in our model, $BED_{30\%\_urethra}$ is 90 Gy with ^{90}Y-avidin, whereas for patients receiving ^{125}I seeds it ranges between 150 and 230 Gy. The rectal DVH is always more favourable with ^{90}Y.
Conclusion The methodology is theoretically feasible and can deliver an effective treatment in T1-T2 prostate cancer. Pharmacokinetic and biodistribution studies in prostate cancer patients are needed for validation.

Keywords Prostate · Avidin · Brachytherapy · ^{90}Y · Monte Carlo · Dosimetry

A related editorial commentary can be found at doi:10.1007/s00259-013-2413-z.

F. Botta · M. Cremonesi · M. E. Ferrari · F. Guerriero · G. Pedroli
Medical Physics Unit, European Institute of Oncology, Milan, Italy

E. Amato
Radiological Sciences Department, University of Messina, Messina, Italy

A. Vavassori
Radiotherapy Division, European Institute of Oncology, Milan, Italy

A. Sarnelli
Radiometabolic Unit and Medical Physics Unit, IRCCS IRST, Meldola, Italy

S. Severi
Radiometabolic and Nuclear Medicine Unit, IRCCS IRST, Meldola, Italy

G. Paganelli (✉)
Division of Nuclear Medicine, European Institute of Oncology, via Ripamonti 435,
20141 Milan, Italy
e-mail: divisione.medicinanucleare@ieo.it

Introduction

According to international recommendations, interstitial permanent brachytherapy with radioactive seeds is considered an established treatment option for low-risk prostate cancer [1, 2]. The possibility of using an ultrasound-guided transperineal technique allows an accurate placement of the seeds and a reliable delivery of the prescribed dose to the prostate. Excellent biochemical and disease-free survival outcomes of a large number of patients have been reported [3].

An optimal absorbed dose distribution is a critical determinant of successful results with permanent seed implantation. Seed migration, in which one or more implanted sources migrate some distance from the proposed location, is a potential well-recognized side effect due to the fact that the radioactive sources are small enough to migrate through the venous plexus surrounding the prostate gland. The increased use of brachytherapy has led to several reports addressing the risk of seed embolization. The most frequent site of migration is the lung [4], although rare migrations have been reported to the heart [5], the kidney [6] and the vertebral venous plexus [7]. Seeds lost to migration detract from the overall dose expected to cover the prostate volume with dosimetric detrimental consequences and a potential change in the effectiveness of treatment. These effects vary in different regions of the prostate: the mean dose to the central region of the gland is roughly independent of the amount of migration, while in the peripheral region it is clearly inversely proportionate to this amount [8, 9].

In the present study, a new therapeutic approach is considered based on multiple injections of ^{90}Y-labelled avidin in small volumes (drops), designed to maximize the uniformity of radiopharmaceutical distribution and, at the same time, the irradiation of the gland. This represents a variation in the approach named intraoperative avidination for radionuclide therapy (IART®) already applied in breast cancer, in which multiple injections of cold avidin are performed in the surgical bed and ^{90}Y-biotin is injected systemically 1 day after surgery. Thanks to the high affinity between avidin and biotin, the radioactivity reaches the avidin in the surgical bed and irradiates the tissues surrounding the excised tumour [10–12].

In the case of stage I–II prostate cancer, pre-targeting with cold avidin is not required as for breast cancer since surgery is not performed. Moreover, using radiolabelled avidin, the required amount of activity is injected into the prostate avoiding unneeded whole-body irradiation. In vitro labelling of avidin can easily be obtained by incubation with a defined amount of ^{90}Y-biotin and then can directly be injected into the prostate as for seed implantation. Details on ^{90}Y labelling of DOTA-biotin have been reported elsewhere [13]. As reported for breast and bladder cancer [11, 14] avidin is retained at the site of injection, probably due to the presence of an oligosaccharide and avidin high isoelectric point as previously described [15].

^{90}Y-avidin can be injected into the prostate using a device similar to that used for seed implantation during interstitial brachytherapy. In the present study, an example of injection strategy, optimized and tailored for a specifically defined geometrical model, is presented. The dosimetric results, obtained by Monte Carlo simulation, are compared to typical performances of ^{125}I seed brachytherapy procedures. Although other radionuclides, such as ^{103}Pd and ^{132}Cs, can be envisaged, our experience is focused on ^{125}I, which is routinely used in our institute.

The aim is to establish whether the theoretical conditions exist to put the proposed method into practice and if the performance—in terms of absorbed dose distribution—can be competitive with respect to ^{125}I seed brachytherapy. Obviously, once the theoretical conditions have been elucidated, a phase I study will be needed to test the practical feasibility, together with a dosimetric analysis tailored to individual patients, as is done for seed implants.

Materials and methods

Theoretical model

Tissue and template modelling

The details of the ^{125}I brachytherapy procedure have been widely described elsewhere [16, 17]. Briefly, the seeds are implanted under biplanar transrectal ultrasonography (TRUS) with or without radioscopic guidance via preloaded needles through predetermined template coordinates, according to the preplan worksheet. The template, fixed on the rectal ultrasound probe, is a 2-D grid, having 13 holes in the horizontal direction and 9 holes in the vertical direction. The distance between two contiguous holes is 5 mm; thus, the template covers a 6×4 cm region.

The design of this study assumes that the ^{90}Y-avidin injections can also be performed by inserting the needle into the template holes, with the same 5-mm step from one position to the next as for the brachytherapy seed implant. The radiopharmaceutical can be released at different depths along each injection line, resulting in a "train" of radioactive drops. A graduated scale on the needle allows the operator to measure the distance between two consecutive drops and release them according to the scheme defined during the treatment planning, by analogy with the ^{125}I seed procedure.

In order to simulate the ^{90}Y treatment and compare different possible designs for delivery, a geometrical model was created to schematically represent the shape and position of the prostate and the organs at risk (urethra and rectum) with respect to the template. The urethra was modelled as a 6 mm diameter cylinder, with the centre coinciding with the central hole of the template. The prostate was represented as a 2 cm radius sphere, concentric with

the urethra, with a concavity in the lower half, to resemble the typical shape of the gland. The total prostate volume was 27.5 cm^3, well representative of the cases indicated for brachytherapy. Finally, the rectum was represented by a cylinder, having a 5 mm thickness wall, with the centre placed 2.3 cm far from the prostate centre. For the evaluation of the rectal absorbed dose, only the wall was taken into account. Figure 1 shows a transaxial representation of the scheme just described, with the central section of the prostate (the one with maximum extension) superimposed on the template.

Injection sites

Starting from the model above, the injection procedure must be optimized in order to balance the therapeutic aim—a uniform and effective irradiation of the gland without side effects—with the procedure feasibility. Namely, it is necessary to optimize the number and the position of the injections, together with the volume of each drop injected, while respecting the constraints on the maximum injectable volume (realistically fixed at 4–5 ml, taking into account the interstitial pressure), maximizing the prostate volume receiving the prescribed absorbed dose and avoiding the risk of urethral involvement. The possibility of ^{90}Y-avidin diffusion after injection also needs to be taken into account.

Considering all these elements, it follows that only a limited number of the template holes can, in practice, be used for ^{90}Y-avidin injection. For example, the holes 5 mm far from the central one are too close to the urethra, so they must be excluded to avoid an unacceptable irradiation of the organ at risk. In particular for the present model, different possible injection strategies were investigated, both considering discrete (drops) and continuous releases along the lines of injection, as well as different positions for the injections and the drops inside the prostate. The absorbed dose maps and the absorbed dose volume histograms (DVH) for the prostate and urethra were compared; the rectal irradiation was very limited in all cases.

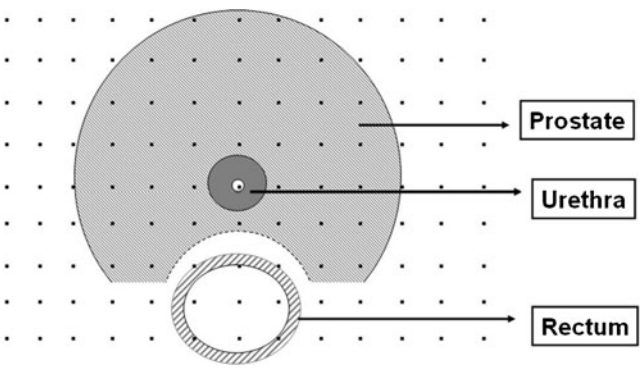

Fig. 1 Transaxial representation of the geometrical model designed to represent the prostate, urethra and rectum and their position with respect to the injection template

The solutions providing the most favourable urethral DVHs that deliver the prescribed absorbed dose to 95 % of the prostate volume as well as the lowest absorbed dose for the urethra and rectum were chosen for this study. The parameters used to compare the urethral DVHs are described in more detail in the "Absorbed dose prescription and constraints" section. With this in mind, the injection strategy that emerged as the most favourable required 22 positions for the injections (Fig. 2a), 13 of which were in the outer ring (black circles) and the remaining 9 in the inner ring (white circles).

Considering a lateral view of the prostate (Fig. 2b), it is evident that a smaller number of activity deliveries can be done along the lines of injections corresponding to the outer ring (bold line), with respect to the inner ring (dotted line), due to the smaller thickness of the prostate along the "z" axis.

In the present model, the optimization procedure leads to performing four deliveries along the injection lines of the inner ring and only two along the injection lines of the outer ring. The depths of injection, according to the coordinate system in Fig. 2b, are: $z=\pm 0.5$ cm in the case of the outer ring and $z=\pm 0.5$ cm and $z=\pm 1.3$ cm in the case of the inner ring. In this way, the distance between two consecutive drops is comparable to the maximum range of ^{90}Y beta particles (11 mm).

Under this hypothesis, a total of 62 drops of ^{90}Y-avidin is assumed to be injected. Considering a 50 μl volume for each drop, the total volume injected into the prostate equals 3.1 ml. As suggested by previous studies of avidin in breast cancer and of monoclonal antibodies in brain tumours, a 2 mm, isotropic avidin diffusion was assumed as a reasonable and likely hypothesis [11, 18]. Thus, it was assumed that, after the injection, the activity included in the 50 μl drop (corresponding to a sphere with 2.3 mm radius) is spread over a spherical volume with 4.3 mm radius. Uniform distribution of activity in the sphere was assumed. The absorbed dose delivered to the prostate and the surrounding tissues is given by the superimposition of the absorbed dose delivered by each drop considered independently.

Absorbed dose computation

To calculate the absorbed dose distribution associated with the whole procedure, the following steps were implemented.

First, the absorbed dose distribution inside and outside a 4.3 mm radius sphere, uniformly filled with ^{90}Y, was calculated by means of Monte Carlo simulation with PENELOPE-2008 code [19]. PENELOPE simulates coupled electron-photon transport in arbitrary materials for a wide energy range, from a few hundred eV to about 1 GeV, on the basis of both numerical databases and analytical cross-sectional models. Details on the code have been

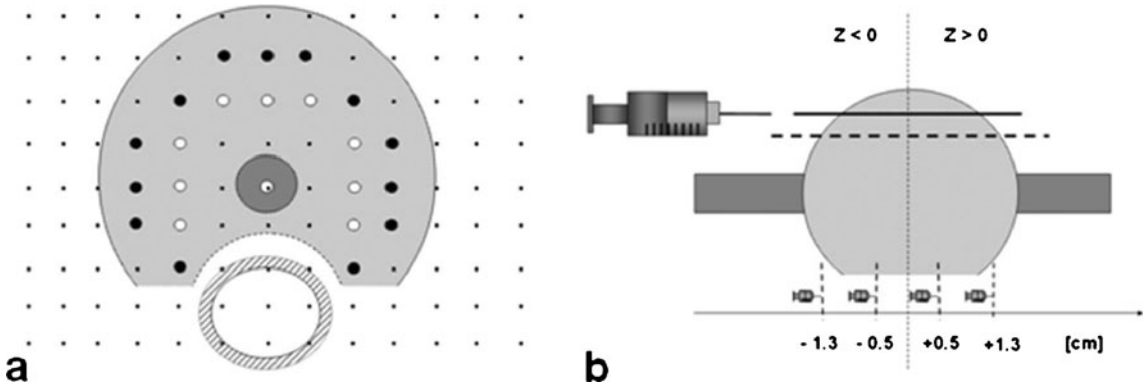

Fig. 2 Transaxial (**a**) and lateral (**b**) representation of the positions identified for ^{90}Y-avidin injection and release of drops

described elsewhere [20]. For monitoring purposes, the same simulation was also performed using GEANT4 version 9.1 [21], a Monte Carlo simulation toolkit originally developed for high energy physics and currently applied also in the field of medical radiation physics [22–24].

For both simulation codes, the absorbed dose was tallied at voxel level in a 111×111×111 matrix of cubical voxels having a 0.5 mm side, with the sphere at the centre of the matrix. In this way, the absorbed dose was evaluated up to more than 2 cm away from the sphere edge, twice the maximum distance covered by ^{90}Y beta particles, allowing the Bremsstrahlung and backscatter contributions to be taken fully into account.

Simulation of 10^7 primary particles was performed, obtaining an absorbed dose uncertainty lower than 1 % inside the sphere and lower than 5 % in the absorbed dose tail, where less than 1 % of the maximum absorbed dose is delivered. Simulation was performed in tissue-equivalent, homogeneous water medium. Particle transport was simulated down to 1 keV threshold, below which the residual energy is assumed to be deposed locally. To include the possibility of injecting drops of different volumes, the same calculation was also repeated for 25 and 100 μl drops. Considering the 2 mm diffusion, this required the simulation of spheres with 3.8 and 4.9 mm radii, respectively.

To complete the calculation, a dedicated program was written in Fortran language. The user is asked to input the coordinates of all the points where a drop is released, and the volume of each drop, choosing among the three volumes available. The dose distributions due to all the injected drops are summed up, and the program provides the dose map over a 191×191×191 voxel matrix (0.5 mm voxel side) having the prostate at its centre [the (0,0,0) point of the coordinate system is in the centre of the prostate]. So, the absorbed dose is evaluated in a cubical volume with a 9.5 cm side, fully including the prostate and the surrounding tissues of concern. In fact, since ^{90}Y is a pure beta emitter, the absorbed dose profile falls very sharply out of the gland, and the cubical volume considered for absorbed dose mapping is more than enough to completely consider every relevant irradiation.

Transaxial images showing the absorbed dose map are produced for a visual representation of the absorbed dose distribution obtained. In addition, the prostate, the urethra and the rectum, according to the geometrical model previously described, are converted into a voxelized form in order to score the dosimetric parameters separately for each organ: minimum, maximum and average absorbed dose, and DVH. The program outputs the dose in terms of dose per unit activity, meaning the total injected activity, summed over all the drops. From this, it is possible to calculate the activity which needs to be injected according to a prescribed dose. At this stage, the eventuality that some of the ^{90}Y-avidin washes out of the prostate can also be accounted for and the injected activity increased accordingly.

Absorbed dose prescription and constraints

^{125}I seed brachytherapy

In the case of ^{125}I seed brachytherapy, absorbed dose prescription and absorbed dose constraints are fixed in terms of minimum absorbed dose to the prostate and maximum absorbed dose to the normal organs, urethra and rectum [25]. Regarding the prostate, at least 95 % of the gland volume must receive an absorbed dose higher than 145 Gy ($D_{95\%}$>145 Gy). Two dose-volume constraints are given for the urethra: as a primary parameter, the absorbed dose received by 10 % of the volume ($D_{10\%}$) must not exceed 150 % of the reference prescription dose ($D_{10\%}$<220 Gy); as a secondary parameter, the absorbed dose received by 30 % of the volume ($D_{30\%}$) must not exceed 130 % of the reference prescription dose ($D_{30\%}$<188 Gy). Finally, in the case of the rectum, the absorbed dose received by a 2 cm^3 volume (D_{2cc}) must not exceed the reference prescription dose (D_{2cc}<145 Gy), and the absorbed dose received by a 0.1 cm^3 volume ($D_{0.1cc}$) must not exceed 150 % of the reference prescription dose ($D_{0.1cc}$<220 Gy).

^{90}Y-avidin therapy

The linear-quadratic model was applied to conveniently translate the dose constraints reported above for the ^{125}I seed brachytherapy to the case of ^{90}Y-avidin irradiation, taking into account the different physical properties of the two sources (summarized in Table 1) and tissue-specific parameters. This invokes the biological effective dose (BED) concept.

According to Fowler et al. [26, 27], in cases of prostate tumour the effects of proliferation can be likely considered negligible due to the slow repopulation; thus, the BED can be calculated as:

$$BED = D \cdot \left(1 + \frac{D}{\frac{\alpha}{\beta}} \cdot \frac{\lambda}{\mu + \lambda}\right) \quad (1)$$

where D is the dose (Gy), α/β (Gy) is the radiobiological parameter—typical of the cell line—that quantifies the change of radiosensitivity when varying the dose fractionation, λ (h^{-1}) is the effective half-life of the radiopharmaceutical within the prostate (equal to the physical decay constant of the radionuclide in case washout is absent) and μ (h^{-1}) is the sublethal damage recovery constant. Under these assumptions, the values of the radiobiological parameters for the prostate tumour are considered to be: α/β= 1.5 Gy and μ=0.36 h^{-1} [26].

Even for the healthy tissues, urethra and rectum, no proliferation occurs, so Eq. 1 is used as well. The values of the radiobiological parameters for the urethra and rectum considered here are those usually reported for healthy tissues: α/β=3 Gy and μ=0.462 h^{-1} [28]. Following these formulations, the ^{125}I absorbed dose constraints were translated into BED constraints and then back into ^{90}Y absorbed dose constraints. The values are summarized in Table 2.

Activity calculation

Two different approaches can be used to calculate the activity to inject starting from the absorbed dose distribution (expressed in terms of Gy×GBq^{-1}). The first one is to calculate the minimum activity required to accomplish with the absorbed dose prescription (i.e. to deliver the prescribed absorbed dose to 95 % of the prostate volume) and verify if the absorbed dose constraints for the organs at risk are also respected. The second approach is to calculate the maximum injectable activity that complies with the absorbed dose constraints for the urethra and to verify whether the absorbed dose prescription is also fulfilled. The absorbed dose to the rectum is so low that it does not represent an issue in any case.

Table 1 ^{125}I and ^{90}Y physical decay properties

	^{125}I seeds	^{90}Y
Emission	X, γ	β^-
Energy	27.4 keV 31.4 keV 35.5 keV	Mean 935 keV – maximum 2.2 MeV
Penetration in water	Linear attenuation coefficient 0.322 cm^{-1}	Range mean 4 mm – maximum 11 mm
Physical half-life	60 days	64 h

Table 2 Absorbed dose constraints for ^{125}I seed brachytherapy translated in terms of BED constraints (linear-quadratic model) and ^{90}Y-avidin absorbed dose constraints

	Prostate	Urethra	Rectum
^{125}I seed dose	$D_{95\%}$>145 Gy	$D_{10\%}$<220 Gy $D_{30\%}$<188 Gy	D_{2cc}<145 Gy $D_{0.1cc}$<220 Gy
BED	$BED_{95\%}$>163 Gy	$BED_{10\%}$<237 Gy $BED_{30\%}$<200 Gy	BED_{2cc}<152 Gy $BED_{0.1cc}$<237 Gy
^{90}Y-avidin dose	$D_{95\%}$>70 Gy	$D_{10\%}$<122 Gy $D_{30\%}$<109 Gy	D_{2cc}<90 Gy $D_{0.1cc}$<122 Gy

Results

The absorbed dose profiles simulated with the PENELOPE code for the 25, 50 and 100 μl spheres are reported in Fig. 3a. Absorbed dose/disintegration (Gy×GBq^{-1}×s^{-1}) is represented as a function of the distance from the sphere centre. Comparing the profiles with those calculated with GEANT4 (Fig. 3b), differences within 2 % were observed inside the spheres, still keeping lower than 7 % in the tail, up to the point where 95 % of the absorbed dose is delivered (R_{95}). The average absorbed dose inside each sphere agrees within ±1 % with the value calculated using the model by Amato et al. [29–31].

An example of the absorbed dose distribution obtained with the injection strategy previously described is reported in Fig. 4 in terms of absorbed dose per unit activity (Gy×GBq^{-1}), superimposed on the prostate and urethral edges. DVHs in terms of absorbed dose per unit activity (Gy×GBq^{-1}) are reported in Fig. 5.

The typical absorbed dose distribution that can be attained with this methodology shows a very high dose in the central region of the prostate, though not uniform, and a very sharp dose decrease when moving towards the urethra and the prostate edge. For the geometrical model considered here, and the hypothesis of no activity washing out the prostate, 0.7 GBq (18 mCi) would be needed following the "minimum required activity" approach, whereas a maximum of 0.86 GBq (23 mCi) could be injected according to the "maximum injectable activity" approach. These values

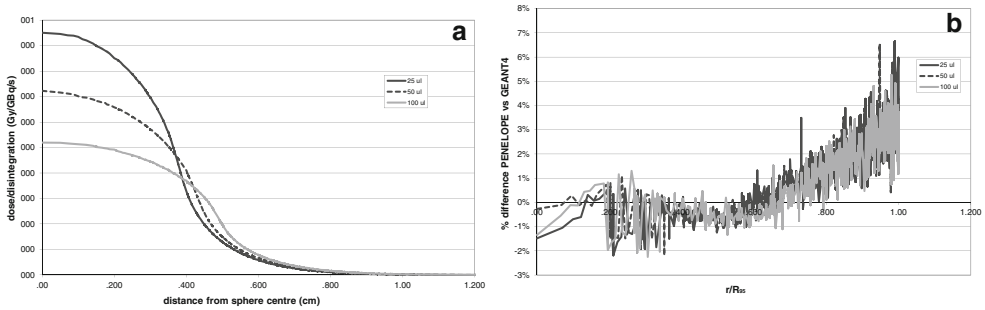

Fig. 3 **a** Absorbed dose profiles calculated with PENELOPE code for 25, 50 and 100 μl spheres uniformly filled with ^{90}Y. Dose/disintegration is represented as a function of the distance from the sphere centre. **b** Percentage difference between the absorbed dose profiles calculated with PENELOPE and GEANT codes, represented as a function of the distance from the sphere centre

give an idea of the activity that could be required for patient treatment.

Table 3 shows the DVH parameters for each case in terms of both ^{90}Y-avidin absorbed dose and BED. By comparison with Table 2 it is evident that the absorbed dose prescription and the absorbed dose constraints are always respected in all cases.

With regard to healthy tissue, both urethral and rectal involvement can be reduced with ^{90}Y-avidin compared to ^{125}I seed brachytherapy. This is certainly always true for the rectum, thanks to the limited path of ^{90}Y beta particles. It is also very likely for the urethra, for the same reason. However, in the case of the urethra the DVH is more dependent on the ^{90}Y distribution, which can be different according to the prostate shape.

To qualitatively assess these issues, a group of ten patients undergoing ^{125}I seeds brachytherapy at our institution was considered. Only those patients with a prostate volume comparable to that of the geometrical model were selected. The best and the worst ^{125}I seed DVHs are shown in Fig. 6 for comparison with the ^{90}Y-avidin model described here (in the case of the minimum required activity approach). The much higher maximum absorbed dose to the prostate obtained with ^{90}Y-avidin is clearly seen (Fig. 6a) in spite of a slightly lower portion of the gland (1–2 % in this example) receiving the prescribed absorbed dose with ^{90}Y-avidin rather than ^{125}I seeds. Figure 6b shows that the global radiation burden to the urethra is lower in the case of ^{90}Y-avidin. However, ^{90}Y-avidin urethral DVH is much less steep than ^{125}I seed DVH when approaching the maximum absorbed dose; this could be critical in the case of ^{90}Y-avidin irradiation since the maximum absorbed dose could be appreciably higher than $D_{10\%}$, which does not happen in the case of ^{125}I irradiation. For this reason, during the ^{90}Y-avidin treatment planning, particular attention must be paid to the urethral DVH even if the absorbed dose constraints are fully respected. The negligible rectal absorbed dose delivered with ^{90}Y-avidin treatment as compared to ^{125}I seed brachytherapy is also made evident (Fig. 6c).

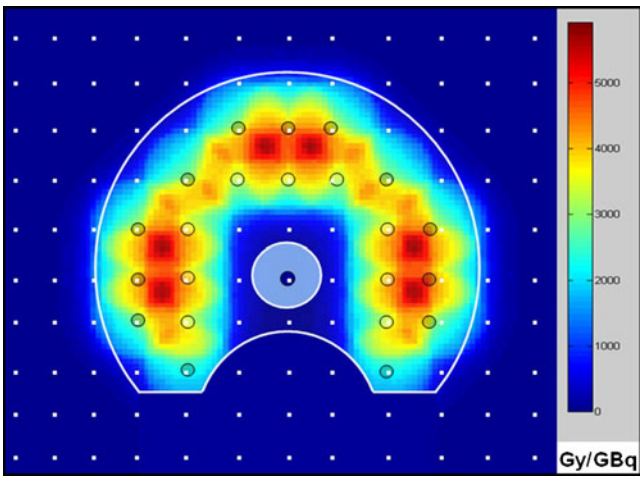

Fig. 4 Transaxial image of the absorbed dose distribution per unit injected activity obtained for the geometrical model and the injection strategy considered for this study

Discussion

Despite the fact that the ^{90}Y-avidin calculations do not refer to a real patient, at this stage these results are enough to confirm that the proposed methodology is theoretically feasible, requiring a reasonable amount of activity, also from the radiation protection point of view, and having the potential to provide good treatment. Obviously, experimental measurements are needed to verify the practical feasibility of the injection procedure and the validity of the assumptions underlying the model. In particular, the amount of avidin diffusion needs to be investigated, as well as the stability of avidin position over time and with every patient position (standing, lying, and moving). To achieve this aim, a diagnostic study can be foreseen with the injection of a tracer activity of radioisotope. A gamma-emitting isotope, such as ^{111}In, could be considered in this phase for imaging purposes to assess the stability/washout from the prostate gland. In fact, images with hepatic and kidney accumulation

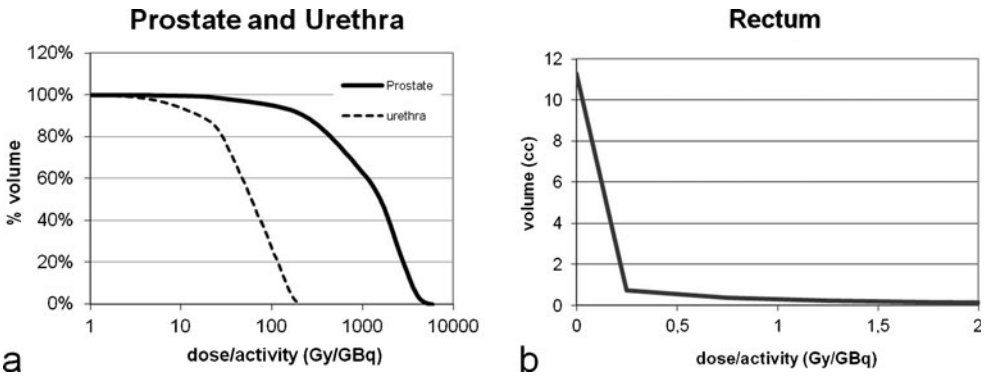

Fig. 5 DVHs for the prostate (*solid line*) and urethra (*dotted line*) (**a**) and rectum (**b**) per unit injected activity obtained for the geometrical model and the injection strategy considered for this study

would indicate that avidin washout occurs, thus allowing us to quantify it [14].

The typical dose distribution obtained with this method, with very steep absorbed dose profiles, is a consequence of the limited range of ^{90}Y beta particles. From the point of view of urethral and rectal safety, this is a major advantage over irradiation with ^{125}I gamma rays and X-rays, which have a longer path. On the other hand, this kind of absorbed dose distribution could lead to under-dosage in some portions of the prostate.

When planning a treatment in clinical practice, for a real patient, it will be fundamental to consider different isotopes and different injection strategies, and to compare the DVHs from competitive plans to identify the best treatment option. Probably, ^{125}I and ^{90}Y therapies would determine the under-dosage of different portions of the gland: typically, the part very proximal to the urethra with ^{90}Y-avidin and a portion of the superior or inferior half of the prostate with ^{125}I seeds. This means that one or the other technique could be more suitable, according to the tumour localization evidenced by the biopsy. Interestingly, prostate tumours appear predominantly in the anterior peripheral zone [32, 33].

Table 3 Prostate, urethra and rectum DVH parameters in cases of ^{90}Y-avidin treatment following the minimum required activity or the maximum injectable activity approach. All data refer to the geometrical model and the injection strategy considered for this study

	Minimum required activity	Maximum injectable activity
Prostate	$BED_{95\%}$=163 Gy	$BED_{95\%}$=247 Gy
	$D_{95\%}$=70 Gy	$D_{95\%}$=90 Gy
Urethra	$BED_{10\%}$=163 Gy	$D_{10\%}$=122 Gy
	$D_{10\%}$=95 Gy	$BED_{10\%}$=237 Gy
	$BED_{30\%}$=91 Gy	$D_{30\%}$=49 Gy
	$D_{30\%}$=62 Gy	$BED_{30\%}$=67 Gy
Rectum	BED_{2cc}<0.2 Gy	BED_{2cc}<0.2 Gy
	D_{2cc}<0.2 Gy	D_{2cc}<0.2 Gy
	$BED_{0.1cc}$=2 Gy	$BED_{0.1cc}$=3 Gy
	$D_{0.1cc}$=2 Gy	$D_{0.1cc}$=3 Gy

As regards the activity to be administered, it can be highlighted that in injecting 0.86 GBq (maximum injectable activity approach) rather than 0.70 GBq (minimum required activity approach), the improvement in terms of target coverage would be minimal, the fraction receiving the prescribed absorbed dose being 96 % rather than 95 %. This is understandable if we take into account the shape of the prostate DVH (Fig. 5a): considering the very slow decrease between 0 and 100 Gy×GBq^{-1}, a fairly high activity variation (as in this case, from 0.7 to 0.86 GBq, +23 % increase) may have very little impact.

The drawback is that a significant improvement in target coverage may be difficult to attain. On the other hand, the advantage of injecting the maximum injectable activity of 0.86 GBq, even assuming a 10–20 % washout, would guarantee more than 0.7 GBq retained in the prostate and thus 95 % target coverage. This is still in accordance with the requirements of the absorbed dose prescription, which accepts a 5 % prostate volume receiving less than the prescribed absorbed dose. Both the maximum injectable activity and the minimum required activity approaches deliver much higher absorbed doses to the gland with respect to ^{125}I brachytherapy, which is very interesting considering the important role of absorbed dose escalation for prostate cancer radiotherapy [28, 34].

There are also radiobiological considerations supporting the use of ^{90}Y-avidin for prostate therapy, especially in cases of tumours with fairly high repopulation rates. It was evidenced in fact that an optimum radionuclide half-life exists according to many parameters, including the tumour repopulation rate, the sublethal damage repair rate, the radiosensitivity and the radiation relative biological effectiveness [35]. When the repopulation rate is high, radionuclides with small half-lives are more desirable, since they deliver a higher initial dose rate and thus better compensate for the repopulation effect. Incorporation of shrinkage effects leads to a further reduction of the optimum half-life, so that the use of short-lived radionuclides is often strongly indicated. In some situations, particularly if the tumour α/β ratio is lower than the normal tissue, the optimum half-life can be lower than 100 h, making ^{90}Y (64 h half-life) preferable to

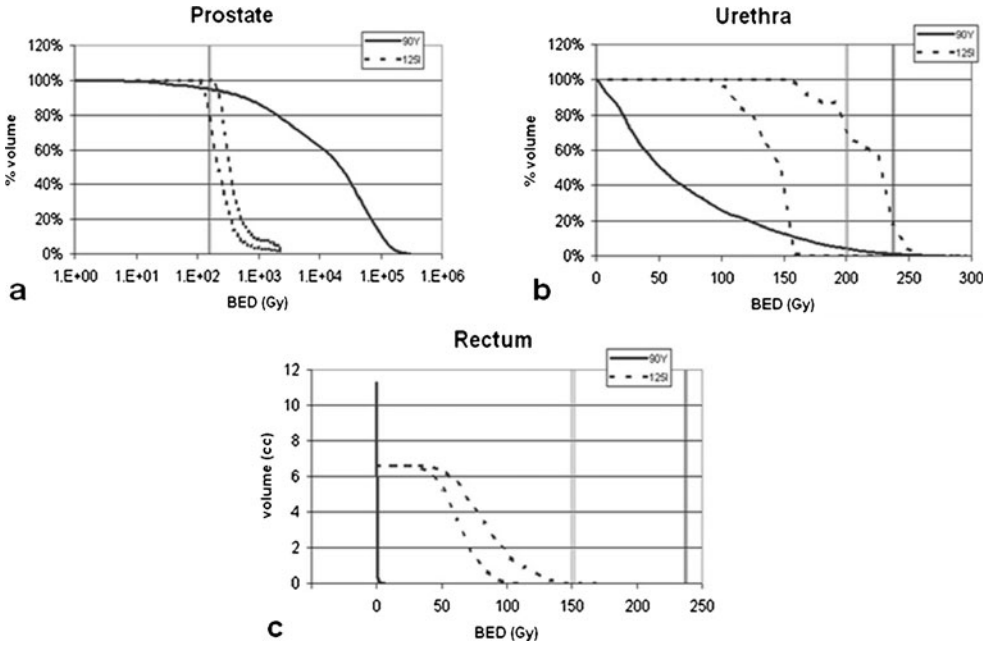

Fig. 6 Comparison between BED VH for the prostate (**a**), urethra (**b**) and rectum (**c**) in the cases of ^{90}Y-avidin (geometrical model, minimum required activity approach) and ^{125}I seed (two extreme patient cases) treatments. *Vertical double lines* symbolize the absorbed dose prescription/dose constraints: **a** $BED_{95\%}$>163 Gy; **b** $BED_{10\%}$<237 Gy, $BED_{30\%}$<200 Gy; **c** BED_{2cc}<152 Gy, $BED_{0.1cc}$<237 Gy

^{125}I (1,440 h half-life). Moreover, a higher dose rate appeared to be desirable to treat higher grade lesions [16]. However, in regards to this it must be highlighted that when repopulation is not negligible, Eq. 1 must be replaced by a more elaborate expression that also takes into account the effects of proliferation. The complete formulation, including a coherent set of radiobiological parameters, has been reported by the AAPM Report No. 137 [25] and by Wang et al. [36]. With this different formulation the prescription absorbed dose to the prostate would be higher than in Table 1 and higher activities would be required, possibly resulting in a less favourable balance between target coverage and urethral sparing as compared to the case with negligible proliferation. To sum up, specific considerations should be done for each case, in order to optimize the treatment not only in terms of DVH comparison, but also from a wider point of view including also radiobiology.

Further room for improvement can be foreseen for the ^{90}Y-avidin methodology, in terms of both urethral sparing and prostate coverage. First of all, the availability of a template with a higher number of holes, separated by less than 5 mm, would allow injecting the avidin more uniformly and getting closer to the urethra, resulting in a more favourable balance between the irradiation of the prostate adjacent to the urethra and urethral sparing. Also, it would be possible to inject activity closer to the prostate edge, and possibly in the tissues immediately outside the prostate, for better irradiation of the outer ring of the gland.

Moreover, with a more crowded template the possibility to use ^{177}Lu-avidin rather than ^{90}Y-avidin could be evaluated. Generally speaking, ^{177}Lu would be preferable for sparing healthy tissue, since the lower energy of its beta particles (maximum energy 0.5 MeV) guarantees an absorbed dose profile steeper than ^{90}Y, and also for its gamma emission producing in vivo imaging. However, with the template now available, it must be excluded in favour of ^{90}Y since the short path of ^{177}Lu beta particles (maximum range 2 mm, mean range 0.2 mm) would also result in a relevant underdosage of the prostate regions between two consecutive drops, unless injecting higher amounts of liquid for a same activity, which is not desirable.

Regarding the possibility of in vivo imaging, interesting results could actually be also obtained with ^{90}Y positron emission tomography (PET) imaging, considering that in this procedure quite a high amount of activity is injected in a small volume [37]. Good quality images could be obtained with reasonable acquisition times, with a resolution—typical of a PET scanner—even better than ^{177}Lu imaging. A sort of post implant study could be done, even if the images probably would not be detailed enough to discriminate prostate and urethral dosimetry.

Last but not least, more advanced radiobiological models could be applied to also take into account the dose heterogeneity and its impact on tumour control probability [38], towards a tailored treatment planning fully accounting for both physical and radiobiological issues.

Conclusion

A new methodology for prostate irradiation has been proposed, based on the injection of ^{90}Y-labelled avidin. The ^{90}Y-avidin treatment proved to be theoretically feasible. In particular, the prescription absorbed dose can be fulfilled respecting the absorbed dose constraints for the organs at risk. The urethral irradiation is likely to be more favourable with ^{90}Y-avidin rather than ^{125}I seeds. The rectum is

completely spared with ^{90}Y-avidin injection. Weak points of the methodology have also been pointed out, allowing us to think about possible strategies for optimization. Pharmacokinetic and biodistribution clinical studies are needed to validate the assumptions underlying this model and to assess the new method in clinical practice.

Conflicts of interest None.

References

1. Ash D, Flynn A, Battermann J, de Reijke T, Lavagnini P, Blank L, et al. ESTRO/EAU/EORTC recommendations on permanent seed implantation for localized prostate cancer. Radiother Oncol 2000;57:315–21.
2. Voulgaris S, Nobes JP, Laing RW, Langley SEM. State-of-the-art: prostate LDR brachytherapy. Prostate Cancer Prostatic Dis 2008;11:237–40.
3. Taira AV, Merrick GS, Butler WM, Galbreath RW, Lief J, Adamovich E, et al. Long-term outcome for clinically localized prostate cancer treated with permanent interstitial brachytherapy. Int J Radiat Oncol Biol Phys 2011;79(5):1336–42.
4. Stone NN, Stock RG. Reduction of pulmonary migration of permanent interstitial sources in patients undergoing prostate brachytherapy. Urology 2005;66:119–23.
5. Schild MH, Wong WW, Vora SA, Ward LD, Nguyen BD. Embolization of an iodine-125 radioactive seed from the prostate gland into the right ventricle: an unusual pattern of seed migration. Radiography 2009;15:179–81.
6. Nguyen BD, Schild SE, Wong WW, Vora SA. Prostate brachytherapy seed embolization to the right renal artery. Brachytherapy 2009;8:309–12.
7. Nakano M, Uno H, Gotoh T, Kubota Y, Ishihara S, Deguchi T, et al. Migration of prostate brachytherapy seeds to the vertebral venous plexus. Brachytherapy 2006;5:127–30.
8. Gao M, Wang JZ, Nag S, Gupta N. Effects of seed migration on post-implant dosimetry of prostate brachytherapy. Med Phys 2007;34(2):471–80.
9. Fuller DB, Koziol JA, Feng AC. Prostate brachytherapy seed migration and dosimetry: analysis of stranded sources and other potential predictive factors. Brachytherapy 2004;3:10–9.
10. Ferrari ME, Cremonesi M, Di Dia A, Botta F, De Cicco C, Sarnelli A, et al. 3D dosimetry in patients with early breast cancer undergoing Intraoperative Avidination for Radionuclide Therapy (IART(®)) combined with external beam radiation therapy. Eur J Nucl Med Mol Imaging 2012;39(11):1702–11.
11. Paganelli G, Ferrari M, Ravasi L, Cremonesi M, De Cicco C, Galimberti V, et al. Intraoperative avidination for radionuclide therapy: a prospective new development to accelerate radiotherapy in breast cancer. Clin Cancer Res 2007;13:5646s–51s.
12. Paganelli G, De Cicco C, Ferrari ME, Carbone G, Pagani G, Leonardi MC, et al. Intraoperative avidination for radionuclide treatment as radiotherapy boost in breast cancer: results of a phase II study with (90)Y-labeled biotin. Eur J Nucl Med Mol Imaging 2010;37:203–11.
13. Urbano N, Papi S, Ginanneschi M, De Santis R, Pace S, Lindstedt R, et al. Evaluation of a new biotin-DOTA conjugate for pretargeted antibody-guided radioimmunotherapy (PAGRIT®). Eur J Nucl Med Mol Imaging 2007;34:68–77.
14. Chinol M, De Cobelli O, Trifirò G, Scardino E, Bartolomei M, Verweij F, et al. Localization of avidin in superficial bladder cancer: a potentially new approach for radionuclide therapy. Eur Urol 2003;44(5):556–9.
15. Yao Z, Zhang M, Sakahara H, Saga T, Arano Y, Konishi J. Avidin targeting of intraperitoneal tumor xenografts. J Natl Cancer Inst 1998;90:25–9.
16. Blasko JC, Mate T, Sylvester JE, Grimm PD, Cavanagh W. Brachytherapy for carcinoma of the prostate: techniques, patient selection, and clinical outcomes. Semin Radiat Oncol 2002;12(1):81–94.
17. Sylvester J, Blasko JC, Grimm P, Ragde H. Interstitial implantation techniques in prostate cancer. J Surg Oncol 1997;66(1):65–75.
18. Hopkins K, Chandler C, Eatough J, Moss T, Kemshead JT. Direct injection of 90Y MoAbs into glioma tumor resection cavities leads to limited diffusion of the radioimmunoconjugates into normal brain parenchyma: a model to estimate absorbed radiation dose. Int J Radiat Oncol Biol Phys 1998;40(4):835–44.
19. Salvat F, Fernández-Varea JM, Sempau J. PENELOPE-2008: A code system for Monte Carlo simulation of electron and photon transport. NEA 6416 ISBN 978-92-64-99066-1. 2008. Available via http://www.oecd-nea.org/science/pubs/2009/nea6416-penelope.pdf.
20. Botta F, Mairani A, Battistoni G, Cremonesi M, Di Dia A, Fassò A, et al. Calculation of electron and isotopes dose point kernels with FLUKA Monte Carlo code for dosimetry in nuclear medicine therapy. Med Phys 2011;38(7):3944–54.
21. Agostinelli S, Allison J, Amako K, Apostolakis J, Araujo H, Arce P, et al. GEANT4 – a simulation toolkit. Nucl Instrum Methods Phys Res A 2003;506:250–303.
22. Carrier JF, Archambault L, Beaulieu L, Roy R. Validation of GEANT4, an object-oriented Monte Carlo toolkit, for simulations in medical physics. Med Phys 2004;31(3):484–92.
23. Amato E, Lizio D, Settineri N, Di Pasquale A, Salamone I, Pandolfo I. A method to evaluate the dose increase in CT with iodinated contrast medium. Med Phys 2010;37(8):4249–56.
24. Amato E, Lizio D, Ruggeri RM, Raniolo M, Campennì A, Baldari S. An analytical model for improving absorbed dose calculation accuracy in non spherical autonomous functioning thyroid nodule. Q J Nucl Med Mol Imaging 2011;55(5):560–6.
25. AAPM Report No. 137, "AAPM recommendations on dose prescription and reporting methods for permanent interstitial brachytherapy for prostate cancer". Report of the AAPM Task Group 137.
26. Fowler J, Chappell RJ, Ritter M. Is α/β for prostate tumors really low? Int J Radiat Oncol Biol Phys 2001;50(4):1021–31.
27. Fowler J, Ritter MA, Fenwick JD, Chappell RJ. How low is the α/β ratio for prostate cancer? In regard to Wang et al., IJROBP 2003;55:194-203. Int J Radiat Oncol Biol Phys 2003;57(2):593–600.
28. Fowler J. The radiobiology of prostate cancer including new aspects of fractionated radiotherapy. Acta Oncol 2005;44:265–76.
29. Amato E, Lizio D, Baldari S. Absorbed fractions in ellipsoidal volumes for $\beta-$radionuclides employed in internal radiotherapy. Phys Med Biol 2009;54:4171–80.
30. Amato E, Lizio D, Baldari S. Absorbed fractions for photons in ellipsoidal volumes. Phys Med Biol 2009;54:N479–87.
31. Amato E, Lizio D, Baldari S. Absorbed fractions for electrons in ellipsoidal volumes. Phys Med Biol 2011;56:357–65.
32. Takashima R, Egawa S, Kuwao S, Baba S. Anterior distribution of stage T1c nonpalpable tumors in radical prostatectomy specimens. Urology 2002;59(5):692–7.
33. Al-Ahamadie HA, Tickoo SK, Olgac S, Gopalan A, Scardino PT, Reuter VE, et al. Anterior-predominant prostatic tumors: zone of origin and pathologic outcomes at radical prostatectomy. Am J Surg Pathol 2008;32(2):229–35.
34. Zelefsky MJ, Pei X, Chou JF, Schechter M, Kollmeier M, Cox B, et al. Dose escalation for prostate cancer radiotherapy: predictors

of long-term biochemical tumor control and distant metastases-free survival outcomes. Eur Urol 2011;60(6):1133–9.
35. Armpilia C, Dale RG, Coles IP, Jones B, Antipas V. The determination of radiobiologically optimized half-lives for radionuclides used in permanent brachytherapy implants. Int J Radiat Oncol Biol Phys 2003;55(2):378–85.
36. Wang JZ, Guerrero M, Li XA. How low is the α/β ratio for prostate cancer? Int J Radiat Oncol Biol Phys 2003;55(1):194–203.
37. Lhommel R, Goffette P, Van den Eynde M, Jamar F, Pauwels S, Bilbao JI, et al. Yttrium-90 TOF PET scan demonstrates high-resolution biodistribution after liver SIRT. Eur J Nucl Med Mol Imaging 2009;36:1696.
38. Strigari L, Orlandini LC, Andriani I, d'Angelo A, Stefanacci M, Di Nallo AM, et al. A mathematical approach for evaluating the influence of dose heterogeneity on TCP for prostate cancer brachytherapy treatment. Phys Med Biol 2008;53:5045–59.